Elastic pulsed wave propagation in media with second- or higher-order nonlinearity. Part I. Theoretical framework

Koen E-A Van Den Abeele[a)]
Los Alamos National Laboratory, EES-4, MS D443, Los Alamos, New Mexico 87545

(Received 8 May 1995; accepted for publication 12 February 1996)

A theoretical model is presented that describes the interaction of frequency components in arbitrary pulsed elastic waves during one-dimensional propagation in an infinite medium with extreme nonlinear response. The model is based on one-dimensional Green's function theory in combination with a perturbation method, as has been developed for a general source function by McCall [J. Geophys. Res. **99** (B2), 2591–2600 (Feb. 1994)]. A polynomial expansion of the equation of state is used in which four orders of nonlinearity in the moduli are accounted for. The nonlinear wave equation is solved for the displacement field at distance x from a symmetric ''breathing'' source with arbitrary Fourier spectrum imbedded in an infinite medium. The perturbation expression corresponds to a higher-order equivalent of the Burgers' equation solution for velocity fields in solids. The solution is implemented numerically in an iterative procedure which allows one to include an arbitrary attenuation function. Energy conservation is investigated in the absence of (linear) attenuation, and the notion of a hybrid (linear and nonlinear) dissipation is illustrated. Examples are provided showing the effect of each term in the perturbation solution on the spectral content of the waveform. Finally, the possibility of creating a parametric array for seismic exploration is briefly considered from a theoretical point of view.

PACS numbers: 43.25.Dc

INTRODUCTION

It is well established that the elastic nonlinear response in some materials is extremely large. Rock in particular displays an enormous nonlinear response and this has been documented in many studies.[1–4] Elastic nonlinearity causes frequency components to mix and energy to be transferred from fundamental frequencies to sum and difference frequencies along the wave propagation path well away from an acoustic or elastic wave source. Traditionally, a perturbation expansion of the equation of state including one nonlinear term has been incorporated into the wave equation to describe this behavior.[5,6] This is the approach of nonlinear acoustics where nonlinear response is generally small relative to materials such as rock.[6,7] However, our work and the work of others has shown that the elementary traditional theory does not describe observations well, or in some instances, not at all.[8,9] Our group is in the process of testing several revised or entirely new theoretical approaches. The two primary approaches are, (1) expanding the equation of state to higher order than is traditionally done, and (2) application of a discontinuous equation of state. The second approach is described in several papers.[8–10] The first approach is the topic of this paper. Back in 1975, Tiersten[11] presented the nonlinear constitutive equations for an isotropic purely elastic solid containing terms up to cubic in the small mechanical displacement gradients. Rather than going over the intense algebra again, we assume the equation of state can be approximated by a higher-order power law expansion of stress as a function of strain.

A. Traditional approach

In this paper we first focus on the effects of elastic nonlinearity, and include attenuation in a later stage. Using the Lagrangian coordinate x and time t, Thurston and Shapiro[12] expressed the differential equation of motion for single mode sound wave propagation in a nonlinear one-dimensional infinite solid in terms of particle displacement u and strain $\epsilon = \partial u/\partial x$ as

$$\rho_0 \frac{\partial^2 u}{\partial t^2} = M_2 \left[1 + \beta \frac{\partial u}{\partial x} + \delta \left(\frac{\partial u}{\partial x} \right)^2 + \cdots \right] \frac{\partial^2 u}{\partial x^2}. \tag{1}$$

Here ρ_0 denotes the unstrained density specific for the medium, $\beta = M_3/M_2$ and $\delta = M_4/M_2$, with M_2, M_3, and M_4 being, respectively, linear combinations of second-order elastic constants, second- and third-order constants, and second-, third-, and fourth-order constants in the direction of propagation. Equation (1) clearly illustrates the hypothesis of a nonlinear modulus-strain relation (or velocity-strain relation since the linear velocity is commonly defined as $c_0 = \sqrt{M_2/\rho_0}$) expressed as a power series in ϵ. Thurston and Shapiro applied a Fourier series expansion of the particle velocity in the simple wave region to obtain an expression for the particle displacement u at distance x assuming an initially pure sinusoidal wave. More recently McCall[13] obtained the same theoretical result using a 1-D power law expansion of stress (σ) versus strain and solving following nonlinear elastic wave equation by use of Green's function

[a)]Also Post-Doctoral Fellow of the Belgian Foundation for Scientific Research, K.U. Leuven Campus Kortrijk, Interdisciplinary Research Center, E. Sabbelaan 53, B-8500 Kortrijk, Belgium.

theory in combination with perturbation methods

$$\rho_0 \frac{\partial^2 u}{\partial t^2} = \frac{\partial \sigma}{\partial x} + S(x,t), \tag{2a}$$

with

$$\sigma(\epsilon) = M_2 \epsilon (1 + \beta' \epsilon + \delta' \epsilon^2 + \cdots)$$
$$= M_2 \frac{\partial u}{\partial x} \left[1 + \beta' \frac{\partial u}{\partial x} + \delta' \left(\frac{\partial u}{\partial x} \right)^2 + \cdots \right] \tag{2b}$$

and $S(x,t)$ being the driver.

The difference between Eqs. (1) and (2) is the identification of β as $2\beta'$ and δ as $3\delta'$. The advantage of McCall's procedure using Green's function theory is that the solution can be written in semianalytical form for any arbitrary source function $S(x,t)$.[13,14]

For most solids the solution of the above equations limited to the first nonlinear term is sufficient to describe their nonlinear response, i.e., only the term in β is needed. The value of the first nonlinearity parameter can be experimentally obtained from a measurement of the amplitude A_2 of the second harmonic displacement (2ω) generated at a distance x from a pure tone (single frequency) source signal

$$\beta = \frac{8 A_2 c_0^2}{A_1^2 \omega^2 x}, \tag{3}$$

where ω is the angular frequency and A_1 is the amplitude of the fundamental frequency.

In some materials it appears that higher-order terms must be employed in order to describe the complete nonlinear response including higher-order harmonics. Some ceramics can be described in this manner.[15–16] Based on perturbation theory, including higher-order nonlinearity (δ term) in the nonlinear equation is not necessary when the amplitude A_3 of the third harmonic (3ω) approximately satisfies

$$A_3 \approx \frac{\beta^2 A_1^3 \omega^4 x^2}{32 c_0^4}. \tag{4}$$

The presence of third harmonic amplitudes for which Eq. (4) is not satisfied may mean that fourth- and perhaps even higher-order elastic coefficients must be taken into account, or that an alternative model with a discontinuous state relation must be considered as mentioned above. A recent study suggests that non-negligible fourth-order elastic coefficients can model the extreme nonlinear behavior in the case of PZT ceramics.[15–16] Na and Breazeale[15] reported a β value of 1500 for PZT ceramics at the Curie temperature and their measured third harmonic amplitudes at room temperature were orders of magnitude larger than predicted by Eq. (4). The same approach may also model the large nonlinear response in Earth materials.[14,17,18] Earth materials are an extreme example of disordered media in which the effective moduli change dramatically as a function of stress due to the presence of compliant features such as microcracks and grain boundaries. Elastic resonance[18] and static stress-strain experiments[19,20] suggest that the ratio of third-order elastic constants to second-order elastic constants in rocks is several orders of magnitude higher than in the case of ordinary materials. Measured values for the first nonlinearity parameter β range from 10^2 to 10^4 whereas typical values between 3 and 15 are observed for most crystalline solids. The observed values for β and the large amplitudes of higher harmonics observed in rock,[17–18] suggest that higher-order elastic coefficients may play an important role. Therefore, if a power law expansion of stress versus strain is a valid assumption, at least the δ term must be taken into consideration in the description of the stress-strain relation for these materials. In this paper we carry out the perturbation expansion including four orders of nonlinearity in the equation of state. In a companion paper (Part II) we compare theoretical to observed results.

Creating a single frequency plane wave source in an experiment is not necessarily straightforward. In order to minimize diffraction effects our group has performed experiments on cylindrical cores using a drive transducer of identical diameter as the core. Pure Young's mode propagation at a single frequency is sought. However, source effects may introduce harmonic distortion of the initial signal. In addition, it is known that the Young's mode in a bar requires some time (or equivalently, some distance) to fully develop its characteristics. Within the distance in which the mode is established in highly nonlinear materials like rock, it may develop a rich harmonic spectrum. In order to account for multiple frequency components in the source we applied the Green's function procedure, developed by McCall, to determine the waveform expression at distance x from a source consisting of an arbitrary pulsed source spectrum. This expression corresponds to a higher-order equivalent of the Burgers' equation solution for velocity fields in solids. It has conceptual clarity and is easy to implement numerically. Analysis of the harmonic content generated along the wave propagation path in the case of a symmetrical source function, and the influence of each term in the power law expansion of the stress-strain relation is illustrated.

Because the general expression is obtained using perturbation theory, it is restricted in its analytical form to small distances from the source. For large distances, the distortion must be calculated in an iterative manner. This will be shown in more detail. Numerical examples will be provided for different numbers of iteration steps showing the convergence of the distorted frequency spectrum as the iteration distance becomes small. From this procedure it will also be shown that rich harmonic spectra can be predicted even if only a minimum number of nonlinearity parameters are taken into account. In addition, the procedure allows us to include any dissipation function accounting for linear attenuation at each iteration step. Finally, the iteration procedure provides a means of accounting for energy conservation in the absence of attenuation. Because nonlinear elasticity implies that energy is transferred between frequency components, we also investigate the notion of ''elastically nonlinear'' attenuation versus ''elastically linear'' attenuation.

The theoretical framework has a number of potential applications. Apart from a pure characterization and classification of the degree of elastic nonlinearity for both normal and disordered solids, we are interested in the sensitivity of nonlinear contributions along the propagation path as a way

of interrogating the compliant nature of the material, such as measurement of consolidation and saturation as well as for symptoms of fatigue or damage. In the case of seismic events in the earth, such as explosions and earthquakes, we seek corrections to the spectrum of seismic waves received at large distances from the source for which we believe that energy is transferred about the spectrum as a function of propagation distance.[14,21] Also the construction of a parametric array in analogy with underwater sound exploration[22–23] is of interest to seismic surveys for directed transmission over a long path length.

I. THEORY

The following theoretical discussion is based on Green's function theory in combination with perturbation analysis as elaborated on in detail by McCall.[13] The one-dimensional nonlinear equation of motion for the displacement field can be obtained by representing stress (σ) as a polynomial expansion in strain (ϵ). The present study takes into account four orders of nonlinearity in this expansion. The resulting one-dimensional nonlinear equation in Lagrangian coordinate x and time t then takes the form

$$\frac{1}{c_0^2}\frac{\partial^2 u}{\partial t^2}=\frac{\partial}{\partial x}\left[\frac{\partial u}{\partial x}\left(1+\beta'\frac{\partial u}{\partial x}+\delta'\left(\frac{\partial u}{\partial x}\right)^2+\eta'\left(\frac{\partial u}{\partial x}\right)^3+\xi'\left(\frac{\partial u}{\partial x}\right)^4\cdots\right)\right]+S(x,t), \tag{5}$$

in which u is the particle displacement, c_0 is the linear velocity, $S(x,t)$ is the expression for the source function, and β', δ', η', and ξ' are the nonlinear parameters. We apply the prime notation in the stress-strain expansion coefficients in order to make the distinction between the more common modulus-strain relation of Thurston and Shapiro. Geophysicists prefer to think in terms of stress whereas velocity is the more favorable terminology in acoustics.

By use of the Green's function

$$G(x,x',\omega)=-\frac{e^{i(\omega/c_0)|x-x'|}}{2i(\omega/c_0)}, \tag{6}$$

for an infinite medium associated with the linear problem, McCall showed that the displacement spectrum at a distance x from the source can be expressed in semianalytical integral form. Applying the same method to Eq. (5) the Fourier transform of the displacement field is given by

$$u(x,\omega)=u^{(0)}(x,\omega)+u^{(1)}(x,\omega)+u^{(2)}(x,\omega)+u^{(3)}(x,\omega)+u^{(4)}(x,\omega), \tag{7}$$

where

$$u^{(0)}(x,\omega)=\int_{-\infty}^{+\infty}dx'\ G(x,x',\omega)\tilde{S}(x',\omega), \tag{8a}$$

with

$$\tilde{S}(s,\omega)=\int_{-\infty}^{+\infty}dt\ S(x,t)e^{i\omega t}, \tag{8b}$$

and $u^{(n)}$ can be calculated by successive approximations, i.e.,

$$u^{(1)}(x,\omega)=\beta'\int_{-\infty}^{+\infty}dx'\ G(x,x',\omega)\int_{-\infty}^{+\infty}\frac{d\omega'}{2\pi}\frac{\partial}{\partial x'}\left[\frac{\partial u^{(0)}}{\partial x'}(x',\omega')\frac{\partial u^{(0)}}{\partial x'}(x',\omega-\omega')\right], \tag{8c}$$

$$u^{(2)}(x,\omega)=2\beta'\int_{-\infty}^{+\infty}dx'\ G(x,x',\omega)\int_{-\infty}^{+\infty}\frac{d\omega'}{2\pi}\frac{\partial}{\partial x'}\left[\frac{\partial u^{(0)}}{\partial x'}(x',\omega')\frac{\partial u^{(1)}}{\partial x'}(x',\omega-\omega')\right]+\delta'\int_{-\infty}^{+\infty}dx'\ G(x,x',\omega)\int_{-\infty}^{+\infty}\int_{-\infty}^{+\infty}\frac{d\omega'}{2\pi}\frac{d\omega''}{2\pi}\frac{\partial}{\partial x'}\left[\frac{\partial u^{(0)}}{\partial x'}(x',\omega')\frac{\partial u^{(0)}}{\partial x'}(x',\omega'')\frac{\partial u^{(0)}}{\partial x'}(x',\omega-\omega'-\omega'')\right], \tag{8d}$$

$$u^{(3)}(x,\omega)=2\beta'\int_{-\infty}^{+\infty}dx'\ G(x,x',\omega)\int_{-\infty}^{+\infty}\frac{d\omega'}{2\pi}\frac{\partial}{\partial x'}\left[\frac{\partial u^{(0)}}{\partial x'}(x',\omega')\frac{\partial u^{(2)}}{\partial x'}(x',\omega-\omega')\right]+\beta'\int_{-\infty}^{+\infty}dx'\ G(x,x',\omega)\int_{-\infty}^{+\infty}\frac{d\omega'}{2\pi}\frac{\partial}{\partial x'}\left[\frac{\partial u^{(1)}}{\partial x'}(x',\omega')\frac{\partial u^{(1)}}{\partial x'}(x',\omega-\omega')\right]+3\delta'\int_{-\infty}^{+\infty}dx'\ G(x,x',\omega)\int_{-\infty}^{+\infty}\int_{-\infty}^{+\infty}\frac{d\omega'}{2\pi}\frac{d\omega''}{2\pi}\frac{\partial}{\partial x'}\left[\frac{\partial u^{(0)}}{\partial x'}(x',\omega')\frac{\partial u^{(0)}}{\partial x'}(x',\omega'')\frac{\partial u^{(1)}}{\partial x'}(x',\omega-\omega'-\omega'')\right]+\eta'\int_{-\infty}^{+\infty}dx'\ G(x,x',\omega)\int_{-\infty}^{+\infty}\int_{-\infty}^{+\infty}\int_{-\infty}^{+\infty}\frac{d\omega'}{2\pi}\frac{d\omega''}{2\pi}\frac{d\omega'''}{2\pi}\frac{\partial}{\partial x'}\left[\frac{\partial u^{(0)}}{\partial x'}(x',\omega')\frac{\partial u^{(0)}}{\partial x'}(x',\omega'')\frac{\partial u^{(0)}}{\partial x'}(x',\omega''')\times\frac{\partial u^{(0)}}{\partial x'}(x',\omega-\omega'-\omega''-\omega''')\right], \tag{8e}$$

and

$$u^{(4)}(x,\omega)=2\beta'\int_{-\infty}^{+\infty}dx'\ G(x,x',\omega)\ \int_{-\infty}^{+\infty}\frac{d\omega'}{2\pi}\frac{\partial}{\partial x'}\left[\frac{\partial u^{(0)}}{\partial x'}(x',\omega')\cdot\frac{\partial u^{(3)}}{\partial x'}(x',\omega-\omega')\right]$$
$$+2\beta'\int_{-\infty}^{+\infty}dx'\ G(x,x',\omega)\int_{-\infty}^{+\infty}\frac{d\omega'}{2\pi}\frac{\partial}{\partial x'}\left[\frac{\partial u^{(1)}}{\partial x'}(x',\omega')\cdot\frac{\partial u^{(2)}}{\partial x'}(x',\omega-\omega')\right]$$
$$+3\delta'\int_{-\infty}^{+\infty}dx'\ G(x,x',\omega)\int_{-\infty}^{+\infty}\int_{-\infty}^{+\infty}\frac{d\omega'}{2\pi}\frac{d\omega''}{2\pi}\frac{\partial}{\partial x'}\left[\frac{\partial u^{(0)}}{\partial x'}(x',\omega')\frac{\partial u^{(0)}}{\partial x'}(x',\omega'')\frac{\partial u^{(2)}}{\partial x'}(x',\omega-\omega'-\omega'')\right]$$
$$+3\delta'\int_{-\infty}^{+\infty}dx'\ G(x,x',\omega)\int_{-\infty}^{+\infty}\int_{-\infty}^{+\infty}\frac{d\omega'}{2\pi}\frac{d\omega''}{2\pi}\frac{\partial}{\partial x'}\left[\frac{\partial u^{(0)}}{\partial x'}(x',\omega')\frac{\partial u^{(1)}}{\partial x'}(x',\omega'')\cdot\frac{\partial u^{(1)}}{\partial x'}(x',\omega-\omega'-\omega'')\right]$$
$$+4\eta'\int_{-\infty}^{+\infty}dx'\ G(x,x',\omega)\int_{-\infty}^{+\infty}\int_{-\infty}^{+\infty}\int_{-\infty}^{+\infty}\frac{d\omega'}{2\pi}\frac{d\omega''}{2\pi}\frac{d\omega'''}{2\pi}\frac{\partial}{\partial x'}\left[\frac{\partial u^{(0)}}{\partial x'}(x',\omega')\frac{\partial u^{(0)}}{\partial x'}(x',\omega'')\right.$$
$$\left.\times\frac{\partial u^{(0)}}{\partial x'}(x',\omega''')\frac{\partial u^{(1)}}{\partial x'}(x',\omega-\omega'-\omega''-\omega''')\right]$$
$$+\xi'\int_{-\infty}^{+\infty}dx'\ G(x,x',\omega)\int_{-\infty}^{+\infty}\int_{-\infty}^{+\infty}\int_{-\infty}^{+\infty}\frac{d\omega'}{2\pi}\frac{d\omega''}{2\pi}\frac{d\omega'''}{2\pi}\frac{d\omega^{(4)}}{2\pi}\frac{\partial}{\partial x'}\left[\frac{\partial u^{(0)}}{\partial x'}(x',\omega')\frac{\partial u^{(0)}}{\partial x'}(x',\omega'')\right.$$
$$\left.\times\frac{\partial u^{(0)}}{\partial x'}(x',\omega''')\frac{\partial u^{(0)}}{\partial x'}(x',\omega^{(4)})\frac{\partial u^{(0)}}{\partial x'}(x',\omega-\omega'-\omega''-\omega'''-\omega^{(4)})\right]. \tag{8f}$$

We are particularly interested in the response of the displacement field at some distance from a source that consists of an arbitrary train of pulsed elastic waves. This will allow us to ignore the near-field effects, and to use the waveform at any position outside the near field as a source input in our model. Because most sources emit some harmonic energy, this approach is also very useful for analyzing the effects of harmonic source distortion on nonlinear wave propagation.

Conforming with our ongoing pulse experiments, we consider the case of a ''breathing'' mode source where the source expands symmetrically about its vertical axis [i.e., $u(-x,t)=-u(x,t)$]. The Fourier transform of the source function in this case can be written as follows:

$$\tilde{S}(x,\omega)=-2\frac{\partial[\hat{\delta}(x)]}{\partial x}2\pi\sum_{n=-\infty}^{+\infty}U_n\hat{\delta}(\omega-n\omega_0) \tag{9}$$

in which $U_n=[U_{-n}]^*$ is a complex number describing the amplitude A_n and phase ϕ_n of the nth harmonic displacement component at $x=0$, i.e., $U_n=-(i/2)A_ne^{i\phi_n}$, and $\hat{\delta}(x)$ is the delta distribution function.

Introducing the source function [Eq. (9)] into Eq. (8a) and working through the immense job of analytically calculating the integrals 8a, c–f we find a general expression describing the harmonic distortion of a pulsed signal propagated over a distance x in an elastic nonlinear medium. In terms of the particle velocity $V_n=-in\omega_0U_n=-n(\omega_0/2)A_n\exp[i\phi_n]$, the perturbation solution for each frequency component is given by

$$V_n(x_0+x)=V_n(x_0)\exp\left[-\frac{n\omega_0}{2Qc_0}|x|\right]+i\omega_0n\frac{x}{|x|}\sum_{l_1=-\infty}^{+\infty}V_{n-l_1}(x_0)V_{l_1}(x_0)W_1(n,l_1)$$
$$-\omega_0n\frac{x}{|x|}\sum_{l_1,l_2=-\infty}^{+\infty}V_{n-l_1-l_2}(x_0)V_{l_1}(x_0)V_{l_2}(x_0)W_2(n,l_1,l_2)$$
$$-i\omega_0n\frac{x}{|x|}\sum_{l_1,l_2,l_3=-\infty}^{+\infty}V_{n-l_1-l_2-l_3}(x_0)V_{l_1}(x_0)V_{l_2}(x_0)V_{l_3}(x_0)W_3(n,l_1,l_2,l_3)$$
$$+\omega_0n\frac{x}{|x|}\sum_{l_1,l_2,l_3,l_4=-\infty}^{+\infty}V_{n-l_1-l_2-l_3-l_4}(x_0)V_{l_1}(x_0)V_{l_2}(x_0)V_{l_3}(x_0)V_{l_4}(x_0)W_4(n,l_1,l_2,l_3,l_4), \tag{10}$$

where n, l_1, l_2, l_3, and l_4 refer to a particular frequency component and to summations indices. Note that W_k denotes the interaction weighting function for the $(k+1)$-fold frequency component interactions. For conciseness we include only the explicit expressions for the functions W_1 and W_2:

$$W_1(n,l_1)=\frac{\beta'}{2c_0^2}|x|, \tag{11a}$$

$$W_2(n,l_1,l_2)=\frac{i}{2c_0^3}\left\{\left[\delta'-\frac{\beta'^2}{2}\left(\frac{2n+l_1+l_2}{n}\right)\right]|x| - i\,\frac{(l_1+l_2)\omega_0}{c_0}\,\frac{\beta'^2}{2}\,|x|^2\right\}. \tag{11b}$$

The weighting functions W_3 and W_4 (and any higher order interaction weighting function) can be calculated using the general formula described in the Appendix. Their leading terms start with terms that are linear with distance and proportional to η' and ξ', respectively.

Equation (10) corresponds to a higher order equivalent of the Burgers' equation solution for particle velocity fields in solids.[24–26] The five parts in this equation correspond to the five terms for each frequency component of the particle velocity distortion over a distance x [equivalent to Eq. (7)]. The first term is the unperturbed frequency component that can be modified by dissipation, introduced in an *ad hoc* manner because there is no attenuation present in the considered nonlinear wave equation. Here we used the common exponential decaying function in which Q_L is a frequency-independent measure of the linear attenuation. All other terms are identified with elastic nonlinear interactions between frequency components and can be considered as corrections to the linear wave propagation theory. Generally the Burger's equation accounts only for interactions between two frequency components [corresponding to the second term in Eq. (7)], whereas the use of Eq. (10) models direct energy mixing between up to five harmonics over the same distance.

II. EXAMPLES AND DISCUSSION

The range of parameters and dimensions used in the illustrations in this paper is inspired by experiments on rock samples performed by our group. Typically, Young's mode velocity ranges between 1800 and 2600 m/s, fundamental frequencies are 5 to 50 kHz, displacement amplitudes range from 10^{-9} to 10^{-6} m (strains of 2.4×10^{-8} to 6.6×10^{-5}), distances extend to 2.0 m and the linear attenuation parameter Q_L varies from 10 to 200. The first and second nonlinearity parameters (β' and δ') have been found to range anywhere between 10 and 10^4 for β' and between 10^3 and 10^9 for δ' based on experimental observations. No experimental evidence has been considered concerning the importance and the values of the higher-order nonlinear parameters η' and ξ'. However, in some cases large harmonics can be observed out to at least the tenth harmonic, 10ω.

In almost all illustrations that will be shown, displacement of one (or more) frequency component(s) is used as the dependent variable. The numerical implementation first converts initial displacement values to velocity, then calculates the distortion for each frequency component over a propagation distance x using Eq. (10), and finally converts distorted velocity back to displacement. We define the order of approximation of the perturbation technique as the number of nonlinear terms taken into account in the calculation of Eq. (7). Note that the mth-order approximation takes into account no more than m orders of nonlinearity, for instance, a second order approximation technique reflects influences of β' and δ' provided these have nonzero values.

In the following we discuss: (1) the implementation of the perturbation solution using an iterative technique and the effects of the iterations on the solution; (2) the influence of source distortion; (3) the effects of the level of approximation used in the perturbation model and the influence of the nonlinearity parameters; (4) the introduction of attenuation and the notion of a local hybrid Q value; (5) the conservation of energy requirement; (6) and some applications. The parameters used as input in the theoretical model are listed in each figure caption.

A. Implementation of the perturbation solution using an iterative technique

Because the general expression is obtained using perturbation theory, it is restricted in its analytical form to small distances x from the source. For large distances L, the distortion must be calculated by iterative procedure.[27] Rather than calculating the distortion directly at a large propagation distance L, we divide the total distance L into N intervals, each of length $x=L/N$. The calculated signal at the beginning of each interval is used as the source for the computation of the waveform and spectrum propagating over the next interval L/N. Figure 1 illustrates the amplitudes of the fundamental and harmonics out to 6ω as a function of the number of iterations using a second-order perturbation technique for a single-frequency drive signal at 15 kHz. Figure 1(a) clearly shows the convergence of the iteration procedure as the number of steps N increases from 1 to 100. This convergence characterizes the stability of the perturbation solution. The bottom portion in Fig. 1(a) illustrates magnified versions of the asymptotic behavior for the first four frequency components. Note that the fundamental amplitude grows as a function of the number of iterations whereas all harmonics decrease in amplitude for larger N. This is because the iterative calculation over smaller and smaller steps reduces the nonlinear correction effects over the total distance. A single iteration causes too much energy to be transferred to the harmonics resulting in an exaggerated correction for the fundamental source frequency component and generation of harmonics that is too large. The more intervals we consider, the more stable the solution will be.

Figure 1(b) provides another view on the harmonic amplitude spectra after 1, 2, and 100 iterations. In the case of a single iteration, we calculate the distortion at a distance of 1 m from the source. Because a second-order perturbation approximation is used only the second and third harmonic amplitudes have nonzero amplitudes which are in this case due to two and threefold interactions of the source frequency with itself. Using two iterations, the distorted spectrum is first calculated at 50 cm from the source resulting in a spec-

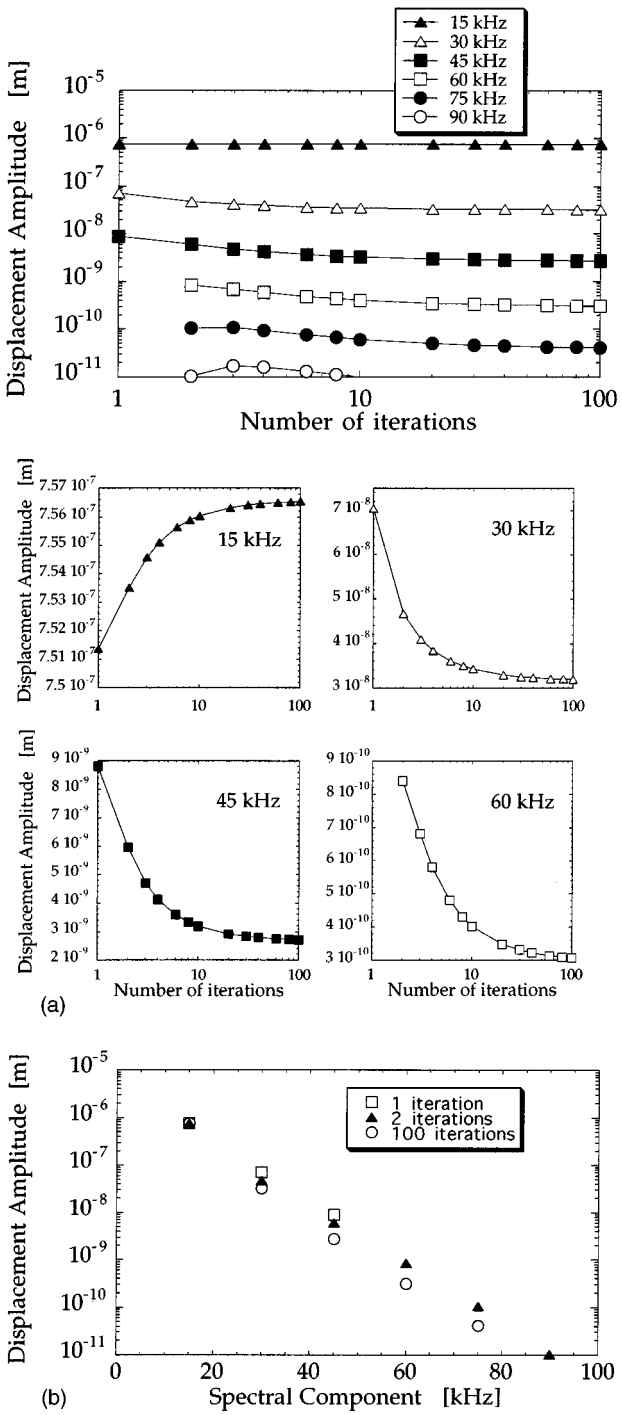

FIG. 1. Convergence of spectral contents for increasing number of iterations (N). Second order perturbation ($u=u^{(0)}+u^{(1)}+u^{(2)}$); $f=15$ kHz, $c_0=2000$ m/s, $Q_L=60$, $L=1$ m, $\beta'=-100$, $\delta'=3\times10^4$; At source: $A_1=1.125\times10^{-6}$ m. (a) Overview of the convergence of all harmonics and detailed behavior of the fundamental, second, third, and fourth harmonics. (b) Total spectrum for one-step, two-step, and 100-step iterations.

trum consisting of a fundamental tone and its second and third harmonic. This multifrequency spectrum is then used as input for the propagation between 50 cm and 1 m, creating a spectrum of nine components. This two-step calculation leads to significant corrections on 2ω and 3ω and to generation of higher harmonics. Further corrections and additional harmonics are obtained by increasing the number of iterations to 100 (equivalent to calculations every 1 cm) until a stable solution is reached. In general, by reducing the step-size and identifying the output of one iteration as the input for the next iteration, it is possible to retrieve a rich and stable spectrum with harmonics of much higher order than the approximation level of the perturbation model considered in the calculations. This is a great advantage of the method.

B. Influence of source distortion

For small distances (only one iteration) and a single-frequency input, the analytical form of the solution given by Eq. (3) suggests easily verifiable relations for experimental observations of the second harmonic A_2 as a function of initial amplitude ($A_2\propto A_1^2$), frequency ($A_2\propto\omega^2$), and distance ($A_2\propto x$).[13,17] At larger distances, these relationships alter somewhat and become more complicated than simple power law dependencies.

Similarly, modification of these predictions occur when a transducer generated second harmonic component is superposed on the fundamental frequency signal at the source. An example is given in Fig. 2 where the predicted dependence of A_2 at some distance from a pure source is compared with the case of a combined fundamental-second harmonic source where the amplitude of the second harmonic equals 5% of the amplitude of the fundamental component. The small second harmonic signal riding on top of the fundamental sinusoidal wave is taken to be out of phase by $\pi/2$. The three plots in Fig. 2 clearly illustrate that the simple power law relationships described by Eq. (3) completely vanish when multiple frequency signals are injected at the source. In this case, the presence of 5% second harmonic at input changes the fundamental input amplitude dependence of the measured displacement amplitude A_2 at 1-m propagation distance from a square-law to a nearly linear dependence [Fig. 2(a)]. Similarly, the behavior as a function of frequency becomes almost constant instead of quadratic [Fig. 2(b)], and the distance dependence starts off at the level of A_2 on input and grows asymptotically toward a linear dependence [Fig. 2(c)]. This result shows that one must be very careful in determining whether or not the source is contaminated before drawing conclusions about nonlinearity parameters or using simple perturbation relations. As also illustrated by Ten Cate *et al.*,[28] a contaminated source may have major consequences on the interpretation of spectral ratios.

C. Effects of the level of approximation used in the perturbation model and the influence of the nonlinearity parameters

From a theoretical point of view, it is also instructive to analyze the contribution of each term in Eq. (7) and in like manner the contribution of each additional nonlinear coefficient in the stress-strain relation. Figure 3 illustrates the corrections due to a successively increased order of approximation in the perturbation solution for a fixed set of four nonzero nonlinearity parameters. Note that an increase of the approximation level in such a case systematically introduces a higher-order nonlinearity parameter in the solution. For

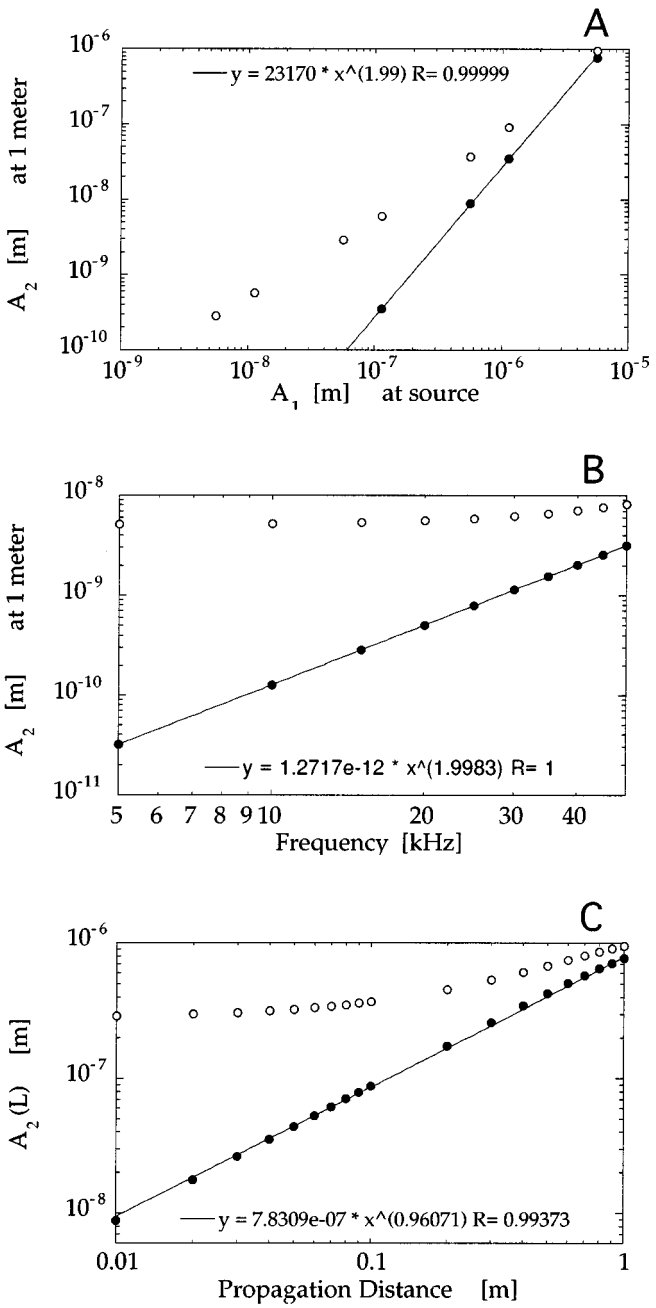

FIG. 2. Functional dependencies of the displacement amplitude of the second harmonic component at 1-m propagation distance from a pure sinusoidal source (filled circles) and a superposed $(f,2f)$-signal (open circles) in which A_2 at the source equals 5% of A_1 and $\phi_2=\pi/2$. Second-order perturbation $(u=u^{(0)}+u^{(1)}+u^{(2)})$; 20 iterations; $c_0=2000$ m/s, no attenuation; $\beta'=-50$, $\delta'=-10^4$. (a) Dependence on the fundamental amplitude at the source. ($f=15$ kHz). (b) Dependence on the fundamental frequency. (At source $A_1=10^{-7}$ m.) (c) Dependence on the propagation distance ($f=15$ kHz; At source $A_1=5.6\times10^{-6}$ m).

instance, increasing the level from order 1 $(u=u^{(0)}+u^{(1)})$ to order 2$(u=u^{(0)}+u^{(1)}+u^{(2)})$ introduces the effects of δ' in the solution. On the other hand, each extra perturbation term $u^{(m)}$ (with $m>0$) depends on all of the lower-order nonlinearity parameters (through the weighting functions), and therefore its contribution for different frequency components can be either negative or positive. Note for instance the decrease of the second and third harmonic and the positive

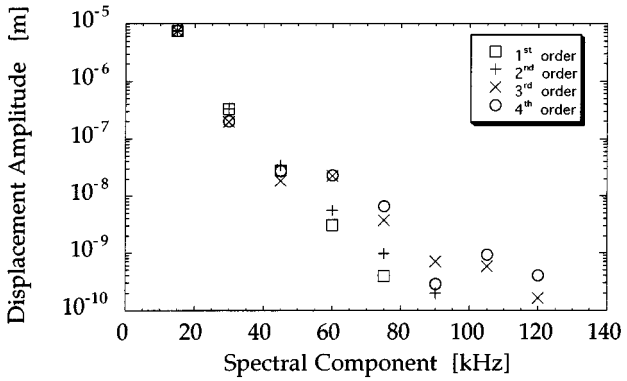

FIG. 3. Nonlinear spectrum for increased order of approximation of the perturbation solution: $f=15$ kHz, $c_0=2000$ m/s, $Q_L=60$, $L=1$ m, $\beta'=-10$, $\delta'=3\times10^2$, $\eta'=2\times10^7$, $\xi'=-3\times10^{10}$. At source: $A_1=1.125\times10^{-5}$ m; 20 iterations. □ 1st order: $u=u^{(0)}+u^{(1)}$, + 2nd order: $u=u^{(0)}+u^{(1)}+u^{(2)}$, × 3rd order: $u=u^{(0)}+u^{(1)}+u^{(2)}+u^{(3)}$, ○ 4th order: $u=u^{(0)}+u^{(1)}+u^{(2)}+u^{(3)}+u^{(4)}$.

contribution to all higher harmonic amplitudes that arise when evaluating the 3rd-order approximation. As can be observed in Fig. 3, the effect of adding higher-order contributions to the theoretical perturbation solution generally lifts up the ''tail'' of the amplitude spectrum while causing only relatively small corrections to the lower harmonics. This result is significant because it can provide guidance as to whether or not higher nonlinearity coefficients are required in the theoretical simulation of a set of experimental data.

In Fig. 4 we plot a related result using the same set of ''linear'' parameters as in Fig. 3. Here we show the effects of computing the 4th-order perturbation solution $(u=u^{(0)}+u^{(1)}+u^{(2)}+u^{(3)}+u^{(4)})$ for a successively increasing number of nonzero nonlinearity coefficients. The iteration number is fixed at 20. We start with the case where all coefficients but β' are zero and proceed by successively adding δ', η', and ξ' contributions. Again we observe that higher-order nonlinearity coefficients modify the spectrum most significantly for higher frequency components. Their contribution can be either positive or negative. Note that the analytical expression of the 4th-order perturbation solution assuming that β' is the only nonzero nonlinear coefficient is

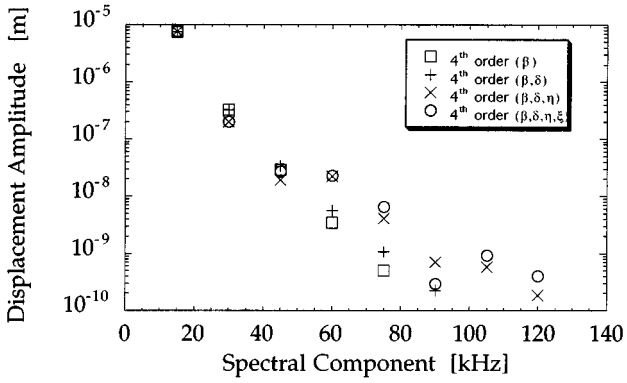

FIG. 4. Fourth-order perturbation solution with increasing number of nonlinearity parameters: $f=15$ kHz, $c_0=2000$ m/s, $Q_L=60$, $L=1$ m; At source: $A_1=1.125\times10^{-5}$ m; 20 iterations. □ $\beta'=-10$, $\delta'=0$, $\eta'=0$, $\xi'=0$; + $\beta'=-10$, $\delta'=3\times10^2$, $\eta'=0$, $\xi'=0$; × $\beta'=-10$, $\delta'=3\times10^2$, $\eta'=2\times10^7$, $\xi'=0$; ○ $\beta'=-10$, $\delta'=3\times10^2$, $\eta'=2\times10^7$, $\xi'=-3\times10^{10}$.

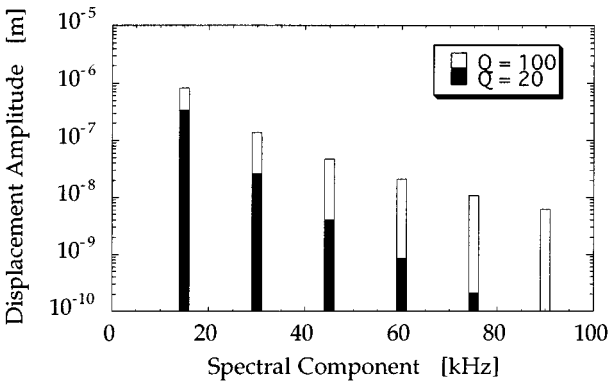

FIG. 5. Displacement spectra for high ($Q_L=20$) and low ($Q_L=100$) linear attenuation. Second-order perturbation ($u=u^{(0)}+u^{(1)}+u^{(2)}$); 50 iterations; $f=15$ kHz, $c_0=2000$ m/s, $L=1$ m, $\beta'=-400$, $\delta'=10^5$; at source: $A_1=1.125\times10^{-6}$ m.

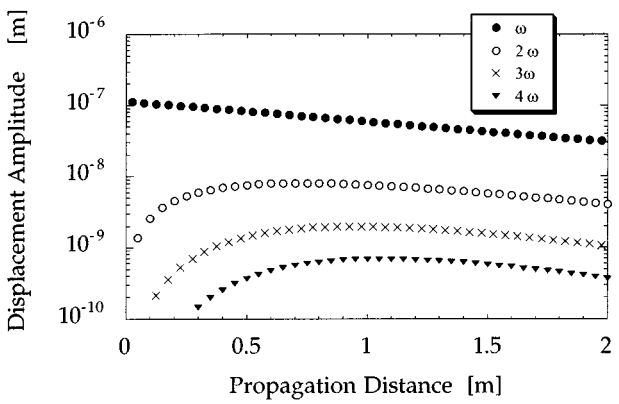

FIG. 6. Fundamental and harmonic displacement amplitudes as a function of distance. Second-order perturbation ($u=u^{(0)}+u^{(1)}+u^{(2)}$); $f=15$ kHz, $c_0=2000$ m/s, $Q_L=40$, $\beta'=-4\times10^3$, $\delta'=-3\times10^7$; at source: $A_1=1.125\times10^{-7}$ m.

not equivalent to restricting Eq. (7) [or Eq. (10)] to the first two terms ($u=u^{(0)}+u^{(1)}$). β' feeds into all higher order terms ($u^{(2)}$, $u^{(3)}$, and $u^{(4)}$) as well. However, due to the iteration procedure there is not much difference in either approach as the iteration by itself will account for the creation of higher harmonics proportional to products of powers of the nonzero nonlinearity parameters in any possible combination. Thus the fact that Figs. 3 and 4 are almost identical is not surprising. This result demonstrates that application of the iteration procedure when using a low level perturbation solution of order m with m nonzero nonlinear coefficients is nearly equivalent to any higher-order approximation that accounts for the same m nonlinearity parameters. In other words, if only two nonlinearity parameters have to be taken into account, a second-order perturbation solution in combination with the iteration procedure will be more than adequate. This conclusion is extremely valuable with respect to computing theoretical simulations which can be very time consuming.

D. Introduction of attenuation and the notion of a local hybrid *Q* value

Apart from obtaining a rich harmonic spectrum with a minimum number of nonlinearity parameters, another advantage of the iteration procedure is that it allows us to include an arbitrary dissipation function accounting for linear attenuation of frequency components at each iteration step. In Eq. (10) we used the common exponential decay function in which Q_L is a frequency independent measure of the linear attenuation. The attenuation coefficient $\alpha_L=-\pi f/Q_L c_0$ depends linearly on frequency as commonly assumed for most solids. However, any attenuation law can be substituted[27] including a Q_L function that varies along the propagation path.

Figure 5 illustrates the effect of high and low Q_L on the spectrum for a drive frequency of 15 kHz at a fixed distance of 1 m. Due to the introduction of attenuation effects at consecutive iteration steps, we observe not only dissipation in the fundamental frequency component, but also significant influences on the generated harmonics. For small Q_L, we observe a smaller amount of energy transfer and thus fewer harmonics. Clearly, knowledge of Q_L for a given experiment is essential when performing theoretical simulations.

Because elastic nonlinearity results in energy being transferred between frequency components, the combination of linear dissipation and nonlinear energy mixing introduces the notion of elastically ''nonlinear'' attenuation as opposed to elastically ''linear'' attenuation. As shown in Fig. 6 nonlinear effects dominate the early wave propagation whereas linear attenuation takes over at large distances. Because harmonics are generated in the medium by multiple frequency coupling, the local hybrid Q value (Q_H) for the nth harmonic including ''linear'' and ''nonlinear'' attenuation, which we define as

$$Q_H^{(n)}(x)=\frac{Q_L^{(n)}(x)\cdot Q_{NL}^{(n)}(x)}{Q_L^{(n)}(x)+Q_{NL}^{(n)}(x)} = \frac{(n\omega/2c_0)\Delta x}{\ln[A_n(x-\Delta x)/A_n(x)]} \quad \text{with } \Delta x \text{ small}, \tag{12}$$

has a distinctive behavior as is illustrated in Fig. 7. As long as nonlinear effects dominate, the value of Q_H is negative for the frequency components that are being generated. Q_H goes asymptotically to $-\infty$ and jumps to $+\infty$ at the distance where nonlinear effects are at their cumulative maximum. This distance differs for each harmonic. Beyond this critical distance attenuation effects dominate and Q_H decreases asymptotically to the value of the linear Q_L characteristic for the medium. For the fundamental frequency component a magnified version of its behavior is shown in the bottom plot. Q_H starts off at Q_L, decreases to a minimum because of the energy loss to higher harmonics, and then increases again asymptotically to the medium constant Q_L at large distances from the source. The hybrid Q value Q_H can be translated to a hybrid attenuation parameter α_H by taking the inverse of Q_H [Fig. 7(b)].

E. Conservation of energy requirement

The introduction of attenuation into the model means that dissipation of energy occurs during propagation. One

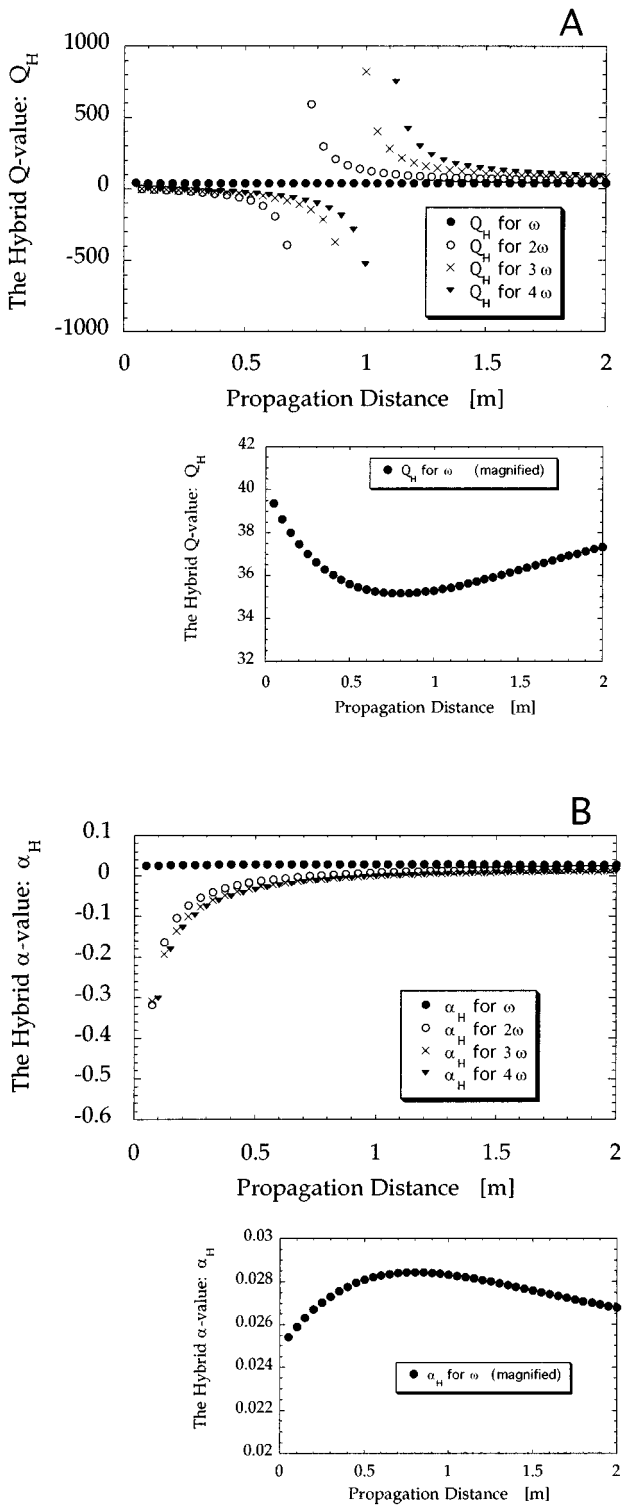

FIG. 7. Behavior of the local hybrid attenuation [Eq. (12)] (a) in terms of Q, (b) in terms of α. Second-order perturbation ($u=u^{(0)}+u^{(1)}+u^{(2)}$); $f=15$ kHz, $c_0=2000$ m/s, $Q_L=40$, $\beta'=-4\times10^3$, $\delta'=-3\times10^7$. At source: $A_1=1.125\times10^{-7}$ m.

can ask the question whether this perturbation approach accounts at all for energy conservation in the absence of attenuation, i.e.:

$$E_0=\sum_{n=-\infty}^{+\infty}[V_n(0)]^2\overset{?}{=}\sum_{n=-\infty}^{+\infty}[V_n(L)]^2=E_L. \tag{13}$$

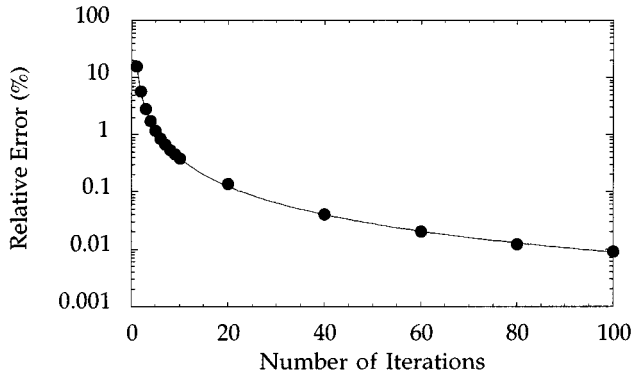

FIG. 8. Relative error (%) of the input–output energy balance as a function of the number of iterations in the absence of attenuation. Second-order perturbation ($u=u^{(0)}+u^{(1)}+u^{(2)}$); $f=15$ kHz, $c_0=2000$ m/s, $L=1$ m, $\beta'=-4\times10^3$, $\delta'=-3\times10^7$; At source: $A_1=1.125\times10^{-7}$ m.

Figure 8 provides an answer to this question. The more iterations, the more accurately energy conservation is satisfied. Using only a single step in the calculation, the excess energy $|(E_L-E_0)/E_0|$ is about 16%. The energy excess decreases monotonically as the number of iterations is increased. A two-step calculation cuts it to 6% and at 100 iterations the error is reduced to 0.01%.

F. Some applications

We emphasize that the theoretical wave propagation model presented here can be applied to any frequency and displacement range. Simulations can extend from ultrasonic acoustic microscopy, over NDE material research in PZT samples on microscales, to ultrasonic MHz-wave propagation in fluids and high-intensity low-frequency seismic waves (Hz range) in Earth materials over several thousands of kilometers. Characterization and classification of the degree of nonlinearity for fluids and solids can lead to accurate information concerning consolidation and saturation conditions within the medium as well as predictions about symptoms of fatigue damage. The more compliant features that exist in a material (microcracks, grain boundaries, and joints) the higher the nonlinear response of the material will be. Because experiments performed by our group indicate that Earth materials are highly nonlinear,[14,17,18] we believe that considerable amounts of energy are transferred from the source frequency spectrum to higher and lower frequencies during seismic events. Recently this hypothesis has been confirmed by observations of Beresnev and Wen.[21] Analysis of detected spectra at different locations could be used to more accurately model explosion and earthquake sources.

To date, we understand much in terms of basic nonlinear phenomena. Various theoretical approaches which are fairly sophisticated have also been developed.[9–11,19,20] However, there have been no real breakthroughs in nonlinear acoustic diagnostic methods for Earth materials because the science of nonlinear elasticity has just arrived at the point where it is now ready to address practical issues. For example, in analogy with ocean acoustic tomography[22–23] the construction of a parametric array in the Earth may signify a major innovation for seismology. A parametric array is created when two collimated, high strain amplitude sound waves of different

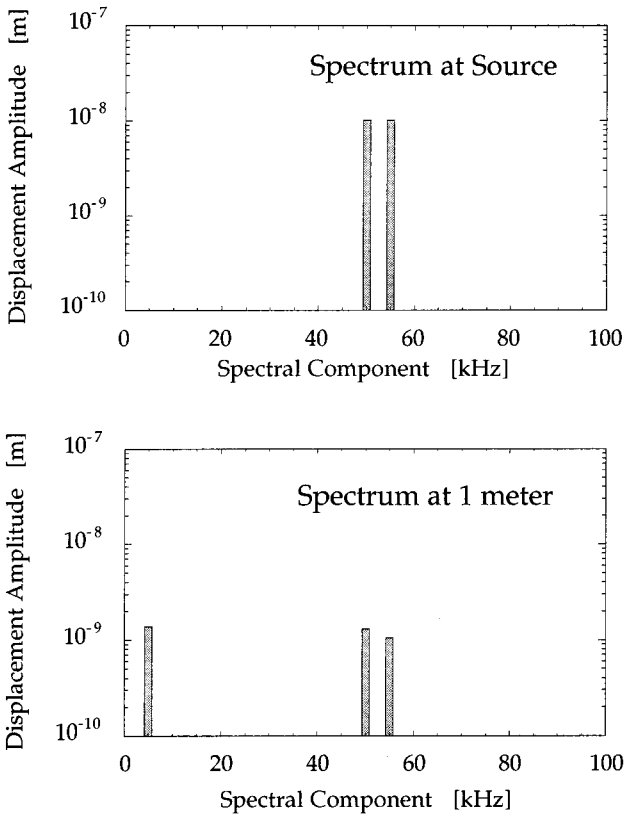

FIG. 9. Simulation of the parametric array principle in highly nonlinear media. Second-order perturbation ($u=u^{(0)}+u^{(1)}+u^{(2)}$); 10 iterations; $c_0=2000$ m/s, $L=1$ m, $Q_L=40$, $\beta'=4\times10^3$, $\delta'=3\times10^7$. At source: $f_{10}=50$ kHz, $A_{10}=1.0\times10^{-8}$ m, $\phi_{10}=0$, and $f_{11}=55$ kHz, $A_{11}=1.0\times10^{-8}$ m, $\phi_{11}=-\pi/2$.

(but close) frequencies are driven simultaneously. The waves interact nonlinearly and generate a frequency at the difference between the two primary wave frequencies. Because this low-frequency wave is nonlinearly generated inside the medium, it does not have the unfavorable spreading properties characteristic to low-frequency beams generated by finite size transducers. The difference frequency signal is fairly well collimated and can be used for transmission over a long path length because it is less attenuated. A simulation using the theoretical framework presented here can give a rough idea of the efficiency of difference frequency collimated beam generation in rock-type materials where values of the nonlinearity parameters can be considerably large. An example is given in Fig. 9. The source is composed of two equal amplitude frequency components having a difference of 5 kHz. While propagating in a nonlinear and dissipative medium, harmonics at all possible sum and difference frequencies are generated. However, due to the increase of attenuation with frequency, only the two source frequency components and the difference frequency are detected at a distance of 1 m. As seen in this example, the amplitude of the 5-kHz component can be comparable with the resultant nonlinearly attenuated amplitudes of the former source. Ideally one would use larger source frequencies to create the parametric array (e.g., 495 and 500 kHz), however, the iterative procedure requires extensive computer memory and CPU time which presently places limitations on the theoretical simulation.

III. CONCLUSION

From Green's function theory and perturbation methods a general expression was derived for describing the nonlinear interaction of frequency components in arbitrary pulsed elastic waves along their propagation path in an infinite medium. Elastic nonlinearity is inserted into the wave equation by assuming a polynomial expansion of the stress-strain relation. The expansion was carried out beyond the second nonlinear term to describe materials with extreme elastic nonlinear behavior. Dissipation can be accounted for due to an iterative implementation of the general expression. The 1-D propagation model can be applied for a broad frequency and amplitude range.

A fundamental question is however if a polynomial expansion of the stress-strain relation is a valid assumption. Hysteretic materials for instance usually have amplitude dependent bi-functional and nonlinear stress-strain curves which complicate the wave propagation model tremendously due to the presence of discontinuous coefficients and the property of discrete memory.[9] Our group is currently working on a model combining nonlinear wave propagation and hysteresis effects. Already in 1988 Nazarov *et al.*[10] realized a discontinuous model was important. However, their stress deformation model should be modified to accommodate recent observations.[19–20]

ACKNOWLEDGMENTS

The author is indebted to P. A. Johnson for careful review of this manuscript. He also thanks K. R. McCall, R. A. Guyer, J. A. Ten Cate, T. J. Shankland, and A. Kadish for helpful discussions and valuable comments. This research is supported by the Office of Basic Energy Science, Engineering and Geoscience under contract W7405-ENG-36 with Los Alamos National Laboratory.

APPENDIX

If $V_n(x_0)$ denotes the nth frequency component of the particle velocity spectrum at distance x_0, the distortion over a distance x further along the propagation path can be calculated as follows:

$$V_n(x_0+x)=V_n^{(0)}(x_0;x)+V_n^{(1)}(x_0;x)+V_n^{(2)}(x_0;x)+V_n^{(3)}(x_0;x)+V_n^{(4)}(x_0;x), \tag{A1}$$

where the mth term in the perturbation solution $(V_n^{(m)}(x_0;x))$ is given by

$$V_n^{(m)}(x_0;x)=i^m n\omega_0 \frac{x}{|x|} \sum_{l_1,\ldots,l_m=-\infty}^{+\infty} V_{[n-\Sigma_{j=1}^m l_j]}(x_0) \times V_{l_1}(x_0)\cdots V_{l_m}(x_0) \cdot \sum_{j=0}^{m} W_j^{(m)}\left(n\omega_0; n-\sum_{j=1}^{m} l_j, l_1,\ldots,l_m\right)\cdot|x|^j. \tag{A2}$$

The coefficients $W_j^{(m)}(\omega;l_0,l_1,\ldots,l_m)$ satisfy following rules (m is the order of perturbation; $j,l_0,l_1,\ldots,l_m$ all are integer summation indices; and ω is the independent variable):

$$W_j^{(m)}(\omega;l_0,l_1,\ldots,l_m)\equiv 0 \quad \text{for } j>m \tag{A3}$$

$$W_0^{(0)}(\omega;l_0)=1/\omega$$
$$W_0^{(m)}(\omega;l_0,l_1,\ldots,l_m)\equiv 0 \quad \text{for } m\neq 0 \tag{A4}$$

$$W_1^{(1)}(\omega;l_0,l_1)=\beta'\ A_1[0,0](\omega;l_0,l_1) \tag{A5}$$

$$W_1^{(2)}(\omega;l_0,l_1,l_2)=2\beta'\ A_1[0,1](\omega;l_0,l_1,l_2)+\delta'\ A_1[0,0,0](\omega;l_0,l_1,l_2)$$
$$W_2^{(2)}(\omega;l_0,l_1,l_2)=2\beta'\ A_2[0,1](\omega;l_0,l_1,l_2) \tag{A6}$$

$$\begin{aligned}W_1^{(3)}(\omega;l_0,l_1,l_2,l_3)&=2\beta'\ A_1[0,2](\omega;l_0,l_1,l_2,l_3)+\beta'\ A_1[1,1](\omega;l_0,l_1,l_2,l_3)+3\delta'\ A_1[0,0,1](\omega;l_0,l_1,l_2,l_3)\\&\quad+\eta'\ A_1[0,0,0,0](\omega;l_0,l_1,l_2,l_3),\\W_2^{(3)}(\omega;l_0,l_1,l_2,l_3)&=2\beta'\ A_2[0,2](\omega;l_0,l_1,l_2,l_3)+\beta'\ A_2[1,1](\omega;l_0,l_1,l_2,l_3)+3\delta'\ A_2[0,0,1](\omega;l_0,l_1,l_2,l_3),\\W_3^{(3)}(\omega;l_0,l_1,l_2,l_3)&=2\beta'\ A_3[0,2](\omega;l_0,l_1,l_2,l_3)+\beta'\ A_3[1,1](\omega;l_0,l_1,l_2,l_3),\end{aligned} \tag{A7}$$

$$\begin{aligned}W_1^{(4)}(\omega;l_0,l_1,l_2,l_3,l_4)&=2\beta'\ A_1[0,3](\omega;l_0,l_1,l_2,l_3,l_4)+2\beta'\ A_1[1,2](\omega;l_0,l_1,l_2,l_3,l_4)\\&\quad+3\delta'\ A_1[0,0,2](\omega;l_0,l_1,l_2,l_3,l_4)+3\delta'\ A[0,1,1](\omega;l_0,l_1,l_2,l_3,l_4)\\&\quad+4\eta'\ A_1[0,0,0,1](\omega;l_0,l_1,l_2,l_3,l_4)+\xi'\ A_1[0,0,0,0,0](\omega;l_0,l_1,l_2,l_3,l_4),\\W_2^{(4)}(\omega;l_0,l_1,l_2,l_3,l_4)&=2\beta'\ A_2[0,3](\omega;l_0,l_1,l_2,l_3,l_4)+2\beta'\ A_2[1,2](\omega;l_0,l_1,l_2,l_3,l_4)\\&\quad+3\delta'\ A_2[0,0,2](\omega;l_0,l_1,l_2,l_3,l_4)+3\delta'\ A_2[0,1,1](\omega;l_0,l_1,l_2,l_3,l_4)\\&\quad+4\eta'\ A_2[0,0,0,1](\omega;l_0,l_1,l_2,l_3,l_4),\\W_3^{(4)}(\omega;l_0,l_1,l_2,l_3,l_4)&=2\beta'\ A_3[0,3](\omega;l_0,l_1,l_2,l_3,l_4)+2\beta'\ A_3[1,2](\omega;l_0,l_1,l_2,l_3,l_4)\\&\quad+3\delta'\ A_3[0,0,2](\omega;l_0,l_1,l_2,l_3,l_4)+3\delta'\ A_3[0,1,1](\omega;l_0,l_1,l_2,l_3,l_4),\\W_4^{(4)}(\omega;l_0,l_1,l_2,l_3,l_4)&=2\beta'\ A_4[0,3](\omega;l_0,l_1,l_2,l_3,l_4)+2\beta'\ A_4[1,2](\omega;l_0,l_1,l_2,l_3,l_4),\end{aligned} \tag{A8}$$

with

$$\begin{aligned}&A_k[N_1,\ldots,N_s](\omega;l_0,\ldots,l_{[s-1+\Sigma_{i=1}^{s}N_i]})\\&=\sum_{p=k-1}^{\Sigma_{i=1}^{s}N_i}\frac{p!}{k!(-2i\omega/c_0)^{p-k+1}}\sum_{n_{s-2}=0}^{N_{s-2}}\cdots\sum_{n_1=0}^{N_1}\left[\prod_{j=1}^{s-2}C_{n_j}^{(j,N_j)}\left(\sum_{r=0}^{N_j}l_{[r+\Sigma_{i=1}^{j-1}(N_i+1)]}\omega_0\right)\right]\\&\quad\cdot\left\{\frac{p+1}{-2i(\omega/c_0)}\sum_{n_{s-1}=\mathrm{Max}\{p+1-\Sigma_{i=1}^{s-2}n_i-N_s,0\}}^{\mathrm{Min}\{p+1-\Sigma_{i=1}^{s-2}n_i,N_{s-1}\}}C_{n_{s-1}}^{(s-1,N_{s-1})}\left(\sum_{r=0}^{N_{s-1}}l_{[r+\Sigma_{i=1}^{s-2}(N_i+1)]}\omega_0\right)\right.\\&\qquad\left.\times C_{p+1-\Sigma_{i=1}^{s-1}n_i}^{(s,N_s)}\left(\omega-\sum_{i=1}^{s-1}\left[\sum_{r=0}^{N_i}l_{[r+\Sigma_{j=1}^{i-1}(N_j+1)]}\omega_0\right]\right)\right.\\&\quad\left.-\frac{1}{2}\sum_{n_{s-1}=\mathrm{Max}\{p-\Sigma_{i=1}^{s-2}n_i-N_s,0\}}^{\mathrm{Min}\{p-\Sigma_{i=1}^{s-2}n_i,N_{s-1}\}}C_{n_{s-1}}^{(s-1,N_{s-1})}\left(\sum_{r=0}^{N_{s-1}}l_{[r+\Sigma_{i=1}^{s-2}(N_i+1)]}\omega_0\right)\right.\\&\qquad\left.\times C_{p-\Sigma_{i=1}^{s-1}n_i}^{(s,N_s)}\left(\omega-\sum_{i=1}^{s-1}\left[\sum_{r=0}^{N_i}l_{[r+\Sigma_{j=1}^{i-1}(N_j+1)]}\omega_0\right]\right)\right\},\end{aligned} \tag{A9}$$

and

$$C_q^{(j,N_j)}(\breve{\omega})=i\,\frac{\breve{\omega}}{c_0}\,W_q^{(N_j)}(\breve{\omega};l_{[\Sigma_{i=1}^{j-1}(N_i+1)]},\ldots,l_{[N_j+\Sigma_{i=1}^{j-1}(N_i+1)]})+(q+1)\cdot W_{q+1}^{(N_j)}(\breve{\omega};l_{[\Sigma_{i=1}^{j-1}(N_i+1)]},\ldots,l_{[N_j+\Sigma_{i=1}^{j-1}(N_i+1)]}). \tag{A10}$$

Finally, the interaction weighting functions used in the text [Eq. (10)] are defined by

$$W_m(n,l_1,\ldots,l_m)=\sum_{j=0}^{m}W_j^{(m)}\left(n\omega_0;n-\sum_{j=1}^{m}l_j,l_1,\ldots,l_m\right)\cdot|x|^j. \tag{A11}$$

[1] F. Birch, in *Handbook of Physical Constants*, edited by S. P. Clark, Jr. (Geol. Soc. Am., CT, 1966), pp. 97–174.
[2] L. A. Ostrovsky, ''Wave processes in media with strong acoustic nonlinearity,'' J. Acoust. Soc. Am. **90**, 3332–3337 (1991).
[3] B. P. Bonner and B. J. Wanamaker, ''Acoustic nonlinearities produced by a single macroscopic fracture in granite,'' in *Review of Progress in Quantitative NDE*, edited by D. O. Thompson and D. E. Chimenti (Plenum, New York, 1991), Vol. 10B, pp. 1861–1867.
[4] P. A. Johnson and P. N. J. Rasolofosaon, ''Nonlinear elasticity and stress-induced anisotropy in rocks,'' J. Geophys. Res. **101**, 3113–3124 (1996).
[5] L. D. Landau and E. M. Lifshitz, *Theory of Elasticity* (Pergamon, Oxford, 1986), 3rd ed.
[6] H. F. Tiersten and J. C. Baumhauer, ''Second Harmonic Generation and Parametric Excitation of Surface Waves in Elastic and Piezoelectric Solids,'' J. Appl. Phys. **45**, 4272 (1974).
[7] M. F. Hamilton, ''Fundamentals and applications of nonlinear acoustics,'' in *Nonlinear Wave Propagation in Mechanics—AMD-77* (The American Society of Mechanical Engineers, New York, 1986).
[8] R. A. Guyer, K. R. McCall, P. A. Johnson, P. N. J. Rasolofosaon, and B. Zinszner, ''Equation of state hysteresis and resonant bar measurements on rock,'' 1995 International Symposium on Rock Mechanics (1995), pp. 177–181.
[9] V. E. Nazarov, L. A. Ostrovsky, I. A. Soustova, and A. M. Sutin, ''Nonlinear acoustics of micro-inhomogeneous media,'' Phys. Earth Planet. Inter. **50**, 65–73 (1988).
[10] K. R. McCall and R. A. Guyer, ''Equation of State and wave propagation in hysteretic nonlinear elastic materials,'' J. Geophys. Res. **99** (B12), 23887–23897 (1994).
[11] H. F. Tiersten, ''Nonlinear electroelastic equations cubic in the small field variables,'' J. Acoust. Soc. Am. **57**(3), 660–666 (1975).
[12] R. N. Thurston and M. J. Shapiro, ''Interpretation of ultrasonic experiments on finite-amplitude waves'' J. Acoust. Soc. Am. **41**, 1112–1125 (1967).
[13] K. R. McCall, ''Theoretical study of nonlinear elastic wave propagation,'' J. Geophys. Res. **99** (B2), 2591–2600 (Feb. 1994).
[14] P. A. Johnson and K. R. McCall, Observation and implications of nonlinear elastic wave response in rock, Geophys. Res. Lett. **21**, 165–168 (1994).
[15] J. K. Na and M. A. Breazeale, ''Ultrasonic nonlinear properties of lead zirconate-titanate ceramics,'' J. Acoust. Soc. Am. **95**, 3213–3221 (1994).
[16] K. Van Den Abeele and M. A. Breazeale, ''Theoretical model to describe dispersive nonlinear properties of Lead Zirconate-Titanate ceramics,'' J. Acoust. Soc. Am. **99**, 1430–1437 (1996).
[17] G. D. Meegan, P. A. Johnson, R. A. Guyer, and K. R. McCall, ''Observations of nonlinear elastic wave behavior in sandstone,'' J. Acoust. Soc. Am. **94**, 3387–3391 (1993).
[18] P. A. Johnson, B. Zinszner, and P. N. J. Rasolofosaon, ''Resonance and nonlinear elastic phenomena in rock,'' accepted for publication in J. Geophys. Res. (1996).
[19] L. B. Hilbert, Jr., T. K. Hwong, N. G. W. Cook, K. T. Nihei, and L. R. Myer, ''Effects of strain amplitude on the static and dynamic nonlinear deformation of Berea sandstone,'' *Rock Mechanics Models and Measurements: Challenges From Industry*, edited by P. P. Nelson and S. E. Laubach (Balkema, Rotterdam, 1994), pp. 497–504.
[20] R. A. Guyer, K. R. McCall, and G. N. Boitnott, ''Hysteresis, discrete memory and nonlinear wave propagation in rock,'' Phys. Rev. Lett. **74**(17), 3491–3494 (1994).
[21] I. Beresnev and K. L. Wen, ''The possibility of observing nonlinear path effects in earthquake-induced seismic wave propagation,'' accepted for publication in Bull. Seismol. Soc. Am. (1996).
[22] P. J. Westervelt, ''Parametric acoustic array,'' J. Acoust. Soc. Am. **26**, 535–537 (1963).
[23] T. G. Muir, ''Nonlinear acoustics: A new dimension in underwater sound,'' in *Science, Technology and the Modern Navy, 30th Anniversary 1946–1976*, edited by E. I. Salkovitz (Department of the Navy, Office of Naval Research, Arlington, VA, 1976), pp. 548–569.
[24] D. T. Blackstock, ''Thermoviscous attenuation of plane, periodic, finite-amplitude sound waves,'' J. Acoust. Soc. Am. **36**, 534–542 (1964).
[25] D. G. Crighton, ''Model equations of nonlinear acoustics,'' Ann. Rev. Fluid Mech. **11**, 11–33 (1979).
[26] D. T. Blackstock, ''Generalized Burgers' equation for plane waves,'' J. Acoust. Soc. Am. **77**(6), 2050–2053 (1985).
[27] M. E. Haran and B. D. Cook, ''Distortion of finite amplitude ultrasound in lossy media,'' J. Acoust. Soc. Am. **73**, 774–779 (1983).
[28] J. A. Ten Cate, K. Van Den Abeele, T. J. Shankland, and P. A. Johnson, ''Laboratory study of linear and nonlinear elastic pulse propagation in sandstone,'' accepted for publication in J. Acoust. Soc. Am. (1996).